Scientific Journal for the Faculty of Science-Sirte University

Journal home page: http://journal.su.edu.ly/index.php/JSFSU/index

DOI: 10.37375/issn.2789-858X

Theoretical Study of the Electronic Structure of Bupivacaine and Lidocaine as Local Anesthetic Agents

Aisha A. AL-abbasi[1]

[1]*Chemistry Department, Science Faculty, Sebha University, Libya*

DOI: https://doi.org/10.37375/sjfssu.v5i1.2573

ARTICLE INFO:

Received: 16 January 2023.

Accepted: 15 March 2025.

Published: 17 April 2025.

Keywords:

Theoretical calculation, Bupivacaine, Lidocaine, DFT calculations, HOMO and LUMO, Quantum parameters, optical properties.

A B S T R A C T

Local anesthetics are widely used pharmaceuticals with numerous therapeutic effects that bind or inhibit other substances that bind to the beta2-adrenergic receptor (beta2 ARs). It was assumed there was a correlation between alkyl chain size of anesthetics and the degree of beta2 AR inhibition required. The findings of this research would utilize quantum computational methods, with special emphasis on DFT and TD-DFT, to study the structural and electronic properties of local anesthetics bupivacaine (B) and lidocaine (L). Important electronic parameters determined include ELUMO and EHOMO, dipole moment (μ), electronegativity (χ), electron affinity (A), chemical hardness (η), chemical softness(S), and ionization potential (I). All these parameters are very significant in understanding the reactivity and interaction of these molecules with biological systems.

1. Introduction

Anaesthesia is an absence of sensation and pain in a certain area due to some chemicals (Nolan, 1997). The orthodontic local anesthesia comes in two groups: esters and amides (Chasteen, 1989). Lidocaine (Figure 1) was first made in 1946, and it is a common local anesthetic and antiarrhythmic drug in the amide group of local anesthetics (Scriabine, 1999). The molecular mass of it is 234.34 g/mol, the chemical formula is C14H22N2O, and it melts at 68 °C. Lidocaine pharmacokinetics demonstrates its rapid onset of action, which usually begins to take effect after four minutes according to the semi-conventional logic so far. The time of its activity is different from one person to another because the dose, the form of administration, and the patient's personal factors all influence the strength and duration of its effect, but usually, it will be between 30 minutes and 3 hours. Lidocaine, being a drug with a relatively brief effect because of its rapid clearance and a small effective window, is the best choice for these treatments, which are not necessary to be prolonged. The toxicity and safety profile of lidocaine are among the most investigated topics. Although lace in the main idiosyncratic, or at the accepted doses, side effects can occur in case of lidozine wrongly point used or at the high concentration (Nolan, 1997).

As noted, lidocaine effectively blocks the sodium ion channels, which are crucial for the initiation and conduction of nerve impulses. By blocking these channels, lidocaine prevents the generation and propagation of nerve impulses, thereby achieving local anesthesia. This mechanism is essential not only in dental and minor surgical procedures but also in the management of certain types of heart arrhythmias due to its effects on cardiac muscle cells (Pharmacists, 2015).

Corresponding author: E-mail: ais.alabbasi@sebhau.edu.ly

Bupivacaine (Figure 1) was synthesized in 1957 for the first time (Hogea et al., 2018; Scriabine, 1999). Bupivacaine is a wide range local anesthetic used in many branches of medicine as it acts for a long time which makes it useful in operations where a long period of anesthesia is required (Balakrishnan et al., 2015). Chemically, the main difference between lidocaine and bupivacaine is that bupivacaine has a longer and more complex chain molecule with the molecular formula $C_{18}H_{28}N_2O$ and molecular weight 288.4 g/mole. The melting point of bupivacaine can be estimated around 258°C that represents the crystalline stable structure which is usually obtain as a white crystalline powder. The structural difference, particularly one which has a long aliphatic chain connected to aromatic ring through amide bond, and not through ester bond, as in some other local anesthetics is responsible for its pharmacological properties.

The structure of bupivacaine allows it to have a higher potency and a longer duration of action compared to lidocaine. These properties make bupivacaine particularly useful for surgeries requiring extended periods of pain relief, thereby reducing the need for repeated administration and minimizing patient discomfort (Scriabine, 1999).

Typically, bupivacaine takes about 15 minutes to start acting and its effects can last anywhere from 2 to 8 hours. This extended duration of action makes it particularly useful for procedures requiring prolonged pain management, which is vital in various medical settings, especially in surgeries where long-lasting analgesia is crucial (Pharmacists, 2015).

Studies have demonstrated that bupivacaine provides effective and longer-lasting pain relief postoperatively, especially in minor surgical procedures performed in outpatient settings (Balakrishnan, 2015). This has established bupivacaine as a preferred choice in many clinical scenarios, despite its slower onset compared to alternatives like lidocaine. The choice between bupivacaine and lidocaine typically depends on the specific medical requirements, patient conditions, and duration of anesthesia required, with bupivacaine often being selected for its prolonged effect (Balakrishnan, 2015).

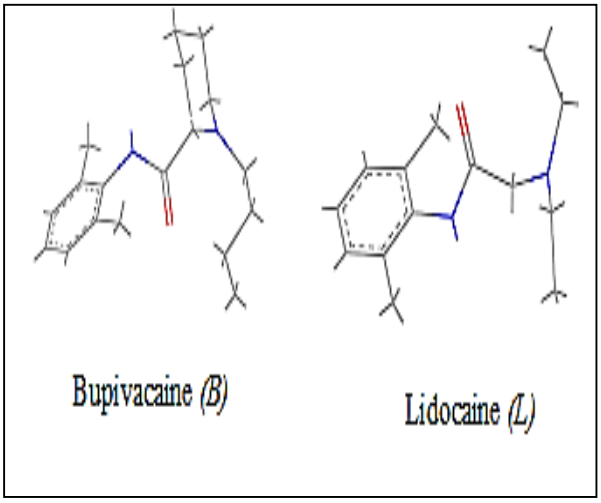

Figure 1: The molecular structures of the explored molecules

Research and molecular simulations have played crucial roles in understanding and predicting its behavior on a molecular level (Al-abbasi & Kassim, 2011; Al-abbasi et al., 2010; Al-Abbassi et al., 2023; Almutaleb & Alabbasi, 2023; Ebenso et al., 2010; Obot et al., 2015; Wazzan, 2014). In light of that, this study typically involves analyzing molecular parameters like electron density, orbital composition, and potential energy surfaces, which can offer insights into how bupivacaine and lidocaine interact at the site of action, and their binding efficiency.

2. Computational details

The computational studies described utilize Materials Studio software version 5.5 from Accelrys for detailed molecular modeling and simulation. This software suite is commonly used in the field of materials science for predicting and understanding the properties of materials both new and existing. In the specific study mentioned, the BLYP functional was applied, which is a form of density functional theory (DFT) that includes a gradient correction to the exchange functional, as proposed by Becke in 1988 and Lee, Yang, and Parr in 1988 (Becke, 1988; Lee et al., 1988).

This function is known for its accuracy in predicting molecular geometries and non-covalent interactions. The calculations were carried out using a double numerical polarization (DNP) basis set, which is a robust set for DFT calculations, providing a good balance between computational cost and accuracy. The use of a generalized gradient approximation (GGA) function enhances the treatment of electron exchange and

correlation effects, critical for accurate molecular simulations (Jon et al., 1996; Perdew et al., 1996). For time-dependent DFT (TD-DFT) simulations, the researchers employed a restricted Hartree-Fock (RHF) method for the ground state. TDDFT is used to investigate the electronic excitations of molecules, which are essential for understanding molecular reactivity, photochemistry, and other dynamics. The RHF method helps to simplify the computational process by assuming that the spatial part of the spin orbitals is the same for electrons with opposite spins, thus reducing the complexity of the electronic calculations (Al-abbasi et al., 2022; Al-abbasi et al., 2012). Such simulations are crucial for predicting how molecules will behave in real-world applications, leading to more directed and efficient experimental designs.

2.2. Theoretical background

This section provides outlines a theoretical framework used in the computational calculation for modeling the electronic properties and reactivity parameters of molecules:

HOMO and LUMO are acronyms for the Highest Occupied Molecular Orbital and the Lowest Unoccupied Molecular Orbital, respectively. They are fundamental in assessing molecular reactivity and stability (Kara et al., 2012; Pearson, 1988; Sastri & Perumareddi, 1994). The energy difference between HOMO and LUMO, known as the band gap (ΔE), directly relates to a molecule's chemical stability and reactivity (Eq. 1).

$$\Delta E = E_{LUMO} - E_{HOMO} \quad (1)$$

Ionization Potential (I) and Electron Affinity (A) are given by equations (2) and (3), where I is the energy required to remove an electron from the HOMO, and A is the energy released when an electron is added to the LUMO. They are calculated from the negative of the energies of the HOMO and LUMO, respectively.

$$I = -E_{HOMO} \quad (2)$$
$$A = -E_{LUMO} \quad (3)$$

Electronegativity (χ), defined in equation (4), is a measure

Electronegativity (χ), defined in equation (4), is a measure of the tendency of an atom or molecule to attract electrons towards itself in a chemical bond. Global hardness (η), (equation 5) is a measure of resistance to change in electron density – a harder molecule is less reactive. Softness (σ) (equation 5), inversely proportional to hardness, is a measure of the ease of electron flow within the molecule (Pearson, 1988).

$$\chi = \frac{I + A}{2} \quad (4)$$
$$\eta = \frac{I - A}{2} \quad (5)$$
$$\sigma = \frac{1}{\eta} \quad (6)$$

Electrophilicity Index (ω, equation 7) quantifies the electrophilicity - the ability of the molecule to accept electrons. It's derived from electronegativity and hardness values (Gece, 2008; Khalil, 2003; Robert G. Parr 1999):

$$\Delta\omega = \frac{\chi^2}{2\eta} \quad (7)$$

Fukui Functions, shown in equations (8), (9), and (10), are used to predict the reactive sites within a molecule (Yang & Mortier, 1986). They indicate where electrons are most likely to be added or removed. Essentially, they help in understanding how a molecule interacts with other species they have been computed by:

$$f^- = (q_N - q_{N-1}) \quad (8)$$
$$f^+ = (q_{N+1} - q_N) \quad (9)$$
$$f^- = \left(\frac{q_{N+1} - q_{N-1}}{2}\right) \quad (10)$$

Here, q = molecule natural charge, N= number of electrons and N+1= an anion, where the LUMO has an extra electron, −1 designates a cation.

Reactivity Descriptors: equations (11& 12) relate to the molecule's overall reactivity towards gaining or losing electrons, calculated by multiplying the Fukui function with the global softness.

$$\sigma^- = (f^-).\sigma \quad (11)$$

$$\sigma^+ = (f^+).\sigma \quad (12)$$

Each of these parameters helps chemists understand and predict how molecules will behave in chemical reactions, which is critical for designing new molecules with desired properties, whether for materials science, pharmaceuticals, or nanotechnology. Computational methods like those described here are crucial for simulating these properties without the need for expensive and time-consuming experimental procedures.

3. Results and discussion

The optimization of the frontier molecular orbitals (FMOs), specifically the highest occupied molecular orbital (HOMO) and the lowest unoccupied molecular orbital (LUMO), focusing on bonds and angles as shown in Figures 2 and 3, provided critical insights into the reactivity of the drug molecule being studied. Further helps in confirming the stability of the molecules under investigation while also providing a clearer view of potential active sites (Costa & Lluch, 1984; Khalifa, 2018). Active sites are crucial for the molecule's activity as they often dictate how the molecule will interact with its environment or with specific targets (Costa & Lluch, 1984; Ebenso et al., 2010; Gece, 2008; Martinez, 2003; Wazzan, 2014).

The calculated high value of HOMO in this study suggests that the drug molecule has a propensity to donate electrons. This is an essential characteristic for molecules intended to interact with biotargets that act as electron acceptors. According to Costa & Lluch and Wazzan (Costa & Lluch, 1984; Wazzan, 2014), molecules with higher HOMO levels are capable of transferring electrons to these acceptor molecules, which often possess low-energy, unoccupied molecular orbitals. This electron donation capability could be advantageous in therapeutic settings where such interactions can influence the biological activity.

Additionally, the gap between these orbitals, denoted as the HOMO-LUMO gap, is a significant descriptor in understanding chemical stability and reactivity. A smaller HOMO-LUMO gap typically signifies that a molecule may be more chemically reactive, prone to electron transfer, and generally less stable. This gap can also influence the electronic properties of the molecule, such as its color and photochemical behavior. On the other hand, a larger gap is indicative of stability and less chemical reactivity, which might be desirable for certain drug characteristics.

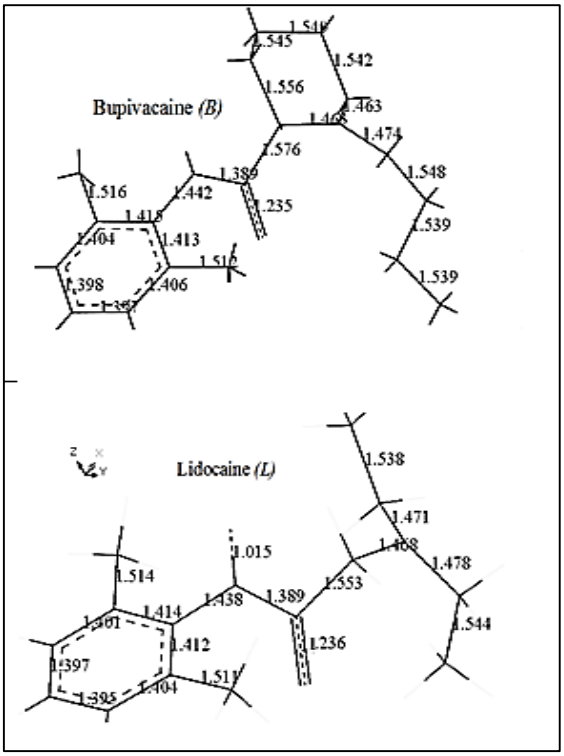

Figure 2: Computed bond length of the optimized structure of the B and L drugs

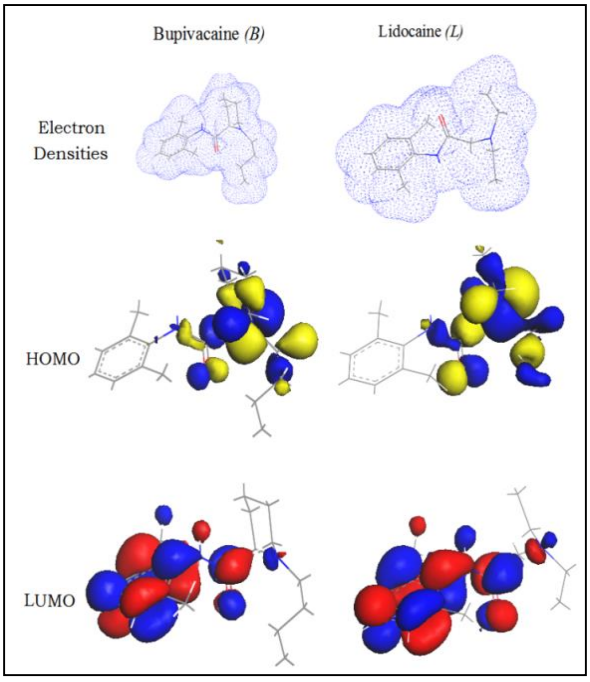

Figure 3: The bupivacaine *(B)* and lidocaine *(L)* computed orbitals

Table 1. Computed parameters for chemical reactivates

Parameters quantities	Unit	Bupiv.	Lido
E_{HOMO}	(eV)	-4.027	-4.236
E_{LUMO}	(eV)	-0.943	-0.874
energy band gap (ΔE)	(eV)	3.084	3.362
Ionization potential l(I)	(eV)	4.027	4.236
Electroaffinity (A)	(eV)	0.943	0.874
Electronegativity (**χ**)	(eV)	2.485	2.555
Global hardness(η)	(eV)	1.542	1.681
global softness (σ)	(eV^{-1})	0.649	0.595
electrophilicity(***ω***)	(eV)	2.002	1.942
dipole moment (μ)	Debye	3.134	3.0057
Binding energy	kcal/mol	-5067.2	-4049.7

Table 1 presents the calculated energy levels of the HOMO and LUMO, showing a clear trend where the EHOMO values for B are higher than those for L. Correspondingly, ELUMO values display an inverse relationship.

This observation is insightful as it indicates a direct correlation between the HOMO energies and the molecule's ability to donate electrons, and inversely with the LUMO energies to accept electrons. Thus, as the EHOMO increases, the molecule becomes a stronger electron donor, enhancing its capacity to interact and bind with the metal surface which typically acts as an electron acceptor. Conversely, lower ELUMO values indicate a stronger tendency to accept electrons, which can also play a critical role in how inhibitors interact with metal surfaces. This dual capability highlights the complex nature of molecular interactions at the surface and provides a route to optimizing the inhibitor design for better corrosion protection efficiency.

Larger energy gaps are associated with higher molecular stability (Al-abbasi, 2021; Belkher, 2019 ; Kara et al., 2012), meaning the molecule is less prone to electron transfer reactions, making it more inert. Conversely, a smaller ΔE facilitates easier electron removal, emphasizing the molecule's reactive nature, which is useful in various applications, such as corrosion inhibition (Mahendra Yadav1, 2014), (Table 1). Regarding electronegativity, a decrease in this value typically suggests an increase in reactivity, as indicated by (Zarrouk et al., 2011). Molecule B exhibits the lowest electronegativity, implying it is more reactive among the compared molecules. This could enhance its effectiveness as an inhibitor by enabling more robust interactions with the metal surface.

Electrophilicity index (ω) serves as another important descriptor in determining the electronic nature of molecules. Typically, entities with lower electrophilicity are better nucleophiles; they are more likely to donate electrons. In contrast, a higher electrophilicity value suggests a strong electrophilic character, meaning the molecule tends to accept electrons readily (Al-abbasi & Kassim, 2011; Khaled, 2009). This distinction helps in understanding the roles molecules can play in various chemical reactions and interactions, particularly in scenarios where electron transfer is significant. Overall, the analysis of EHOMO, ELUMO, ΔE, electronegativity, and electrophilicity provides a comprehensive understanding of molecular reactivity, stability, and interaction capabilities, fostering informed uses in specific applications such as corrosion inhibitors or reactive intermediates in synthesis processes.

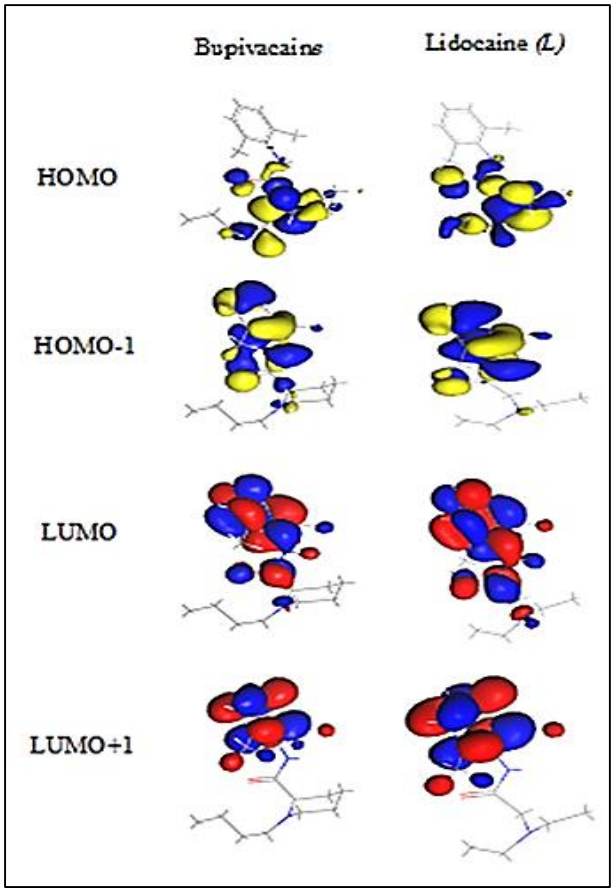

Figure 4: Orbitals distributions computed at the Dmol³ level

The information provided suggests that among the different molecules considered, molecule B has the lowest molecular hardness and highest softness, indicating that it is generally more reactive. This is supported by the values of the Fukui function indices presented in Table 2, where higher values indicate sites of increased reactivity towards electrophilic attack.

Table 2. Fukui Indices for Electrophilic Attack at O1 and N1 atoms

	B	L
at O1 of C=O	0.063	0.107
N1 of N-H	0.203	0.185

Examining the specific sites within these molecules, the technical data for electrophilic attack at atoms O1 (oxygen in the carbonyl group, C=O) and N1 (nitrogen in the amide group, N-H) demonstrates significant differences between molecules B and L. For O1, molecule B has a relatively lower Fukui index (0.063) compared to molecule L (0.107), suggesting that the oxygen in the carbonyl group of molecule B is less susceptible to electrophilic attack compared to molecule L. In contrast, for the nitrogen atom N1, the Fukui function index is higher in molecule B (0.203) than in molecule L (0.185). This indicates that the nitrogen in the amide group of molecule B is a more reactive site for electrophilic attack compared to molecule L. This aligns with the overall higher softness and lower hardness of molecule B, as the nitrogen atom appears to be a particularly favorable site for reaction.

TDDFT Calculations

The TD-DFT (Time-dependent Density Functional Theory) calculations and analyses presented in Figures 4 and 5 reveal crucial insights into the electronic properties of bupivacaine (B) and lidocaine (L). These compounds, when analyzed under vacuum conditions via simulated UV-Vis absorption spectra, exhibit significant details about their electronic transitions.

The simulated absorption spectra as delineated in Figure 5 highlight two low-intensity absorption bands within the 300-400 nm range, which correspond to the n→π* transitions. Such transitions typically arise when non-bonding electrons (n-electrons) are excited to anti-bonding π* orbitals, indicating potential reactivity or certain chemical behavior under light exposure. The additional band located around 250 nm is indicative of π→π* transitions, where electrons within bonding π orbitals are excited to corresponding anti-bonding π* orbitals.

The n→π transitions of the B molecule were redshifted to higher wavelengths compared to the *n→π* transitions of the l molecule, which supports the hypothesis of the small band gap in the B molecule. This transition is important because it usually involves the conjugated systems in the molecules, which affects their color and photoreactivity.

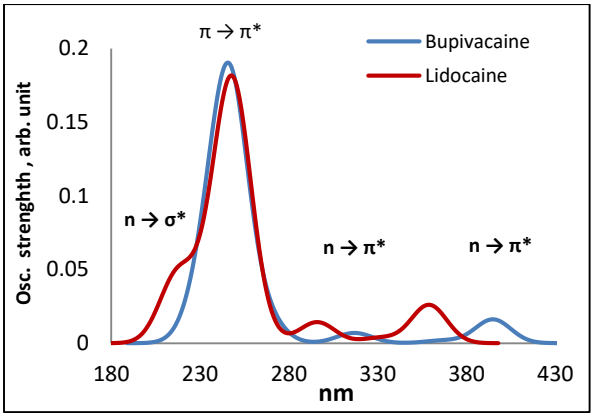

Figure 5: Calculated absorption spectra of bupivacaine *(B)* and lidocaine *(L)* in vacuum

4. Conclusions

Based on the theoretical study conducted on bupivacaine and lidocaine, which are both commonly used as local anesthetic agents, several important conclusions can be drawn from the DFT (Density Functional Theory) and TD-DFT (Time-Dependent Density Functional Theory) calculations:

1. Bupivacaine displayed higher reactivity compared to lidocaine, which is evidenced by its higher EHOMO and lower ELUMO. The smaller energy gap in bupivacaine suggests that it can more readily participate in chemical interactions and reactions.
2. The HOMO orbitals of both bupivacaine (B) and lidocaine (L) were found to be mainly constituted by the aliphatic parts of the molecules, indicating that these regions play a significant role in electron donation.
3. The LUMO orbitals, in contrast, are predominantly located on the aromatic regions with notable contributions from the carbonyl (C=O) groups of the amide moieties. These characteristics suggest

areas on the molecules that are likely acceptors in interactions involving electron transfer.

4. The optical transition analysis revealed three distinct types of electronic transitions of n→π*, π→π*, and potentially σ→π*. The presence of these transitions indicates various pathways for electronic excitations under light absorption, each contributing differently to the spectral properties of these compounds.
5. These findings not only enhance the understanding of the electronic and optical properties of bupivacaine and lidocaine but also potentially aid in the design and development of new anesthetic agents with optimized properties.
6. The differences in reactivity and electronic transitions between the two drugs might influence their pharmacological efficiencies and stabilities, which could be significant for clinical applications.

Acknowledgement

The Chemistry Department at Sebha University is acknowledged.

References

Al-abbasi, A., and Shana, I. . (2021). Corrosion Inhibition of Mild Steel in Acidic Media by Expired Carbimazole Drug. *Journal of Pure & Applied Sciences*, *20*(2), 176–180. https://doi.org/https://doi.org/10.51984/jopas.v20i2.1646

Al-abbasi, A., & Kassim, M. (2011). 1-Ethyl-1-methyl-3-(2-nitrobenzoyl)thiourea. *Acta Crystallographica Section E*, *67*(7), o1840. https://doi.org/doi:10.1107/S1600536811024652

Al-abbasi, A., Tahir, M., Kayed, S., & Kassim, M. (2022). Synthesis, characterisation and biological activities of mixed ligand oxovanadium (IV) complexes derived from N,N-diethyl-N′-para-substituted-benzoylthiourea and hydrotris(3,5-dimethylpyrazolyl)borate [https://doi.org/10.1002/aoc.6607]. *Applied Organometallic Chemistry*, *36*(4), e6607. https://doi.org/https://doi.org/10.1002/aoc.6607

Al-abbasi, A. A., Mohamed Tahir, M. I., & Kassim, M. B. (2012). N-(Pyrrolidin-1-ylcarbothioyl)benzamide. *Acta Crystallographica Section E*, *68*(1), o201. https://doi.org/doi:10.1107/S1600536811053694

Al-abbasi, A. A., Yarmo, M. A., & Kassim, M. B. (2010). N-[(Piperidin-1-yl)carbothioyl]benzamide. *Acta Crystallographica Section E*, *66*(11), o2896. https://doi.org/doi:10.1107/S160053681004170X

Al-Abbasi, A. A., Kayed, S. F., & Kassim, M. B. (2023). Spectral, theoretical, physicochemical and corrosion inhibition studies of ortho-, meta- and para-hydroxyphenyl-benzoylthiourea ligands. *Inorganic Chemistry Communications*, *156*, 111155. https://doi.org/https://doi.org/10.1016/j.inoche.2023.111155

Almutaleb, A. A. A., & Alabbasi, A. A. (2023). Synthesis, characterization and computational studies for (2′S*,3R*,3′S*,8a′R*)-2′,3′-bis(ethoxycarbonyl)-2-oxo-2′,3′-dihydro-8a′H-spiro[indoline-3,1′-indolizine]-6′-carboxylic acid and some derivatives. *Journal of Physical Organic Chemistry*, *36*(2), e4452. https://doi.org/https://doi.org/10.1002/poc.4452

Balakrishnan, K., Ebenezer, V., Dakir, A., Kumar, S., & Prakash, D. (2015). Bupivacaine versus lignocaine as the choice of locall anesthetic agent for impacted third molar surgery a review. *Journal of Pharmacy and Bioallied Sciences*, *7*(Suppl 1). https://journals.lww.com/jpbs/fulltext/2015/07001/bupivacaine_versus_lignocaine_as_the_choice_of.64.aspx

Balakrishnan, K., Ebenezer, V., Kumar, A., and Prakash, D.,. (2015). Bupivacaine versus lignocaine as the choice of locall anesthetic agent for impacted third molar surgery a review. *J Pharm Bioallied Sci.*, *7*, S230–S233.

Becke, A. D. (1988). Density-functional exchange-energy approximation with correct asymptotic behavior. *Physical Review A*, *38*(6), 3098. http://link.aps.org/doi/10.1103/PhysRevA.38.3098

Belkher, N., Al-abbasi, A., and Zidan, M. . (2019). Potentiometric Studies on Stability Constant of the Complexes of SomeEssential Transition Metal Ions with L-Valine. *Journal of Pure & Applied Science 13*(3), 59-63.

Chasteen, J. E. (1989). *Essentials of Clinical Dental Assisting*. Mosby. https://books.google.com.ly/books?id=nRtqAAAAMAAJ

Costa, J. M., & Lluch, J. M. (1984). The use of quantum mechanics calculations for the study of corrosion inhibitors. *Corros Sci*, *24*. https://doi.org/10.1016/0010-938x(84)90113-6

Ebenso, E. E., Isabirye, D. A., & Eddy, N. O. (2010). Adsorption and quantum chemical studies on the inhibition potentials of some thiosemicarbazides for the corrosion of mild steel in acidic medium. *Int J Mol Sci*, *11*. https://doi.org/10.3390/ijms11062473

Gece, G. (2008). The use of quantum chemical methods in corrosion inhibitor studies. *Corros Sci*, *50*. https://doi.org/10.1016/j.corsci.2008.08.043

Hogea, B., Andor, B., Totorean, A., Hogea, L., Nussbaum, L., Bistrian, A., Sandesc, M., Folescu, R., Stanciulescu, M., Dobrin, R., Boanca, M., & Jr, P. (2018). Use of Intraoperative Analgesic and Anesthetic Substances by Intramuscular Infiltrations during Hip Surgery for Postoperative Pain Monitoring. *Revista de Chimie*, *69*, 3530-3532. https://doi.org/10.37358/RC.18.12.6785

Jon, B., Alain, K., & Bernard, D. (1996). *The generation and use of delocalized internal coordinates in geometry optimization* (Vol. 105). AIP. http://dx.doi.org/doi/10.1063/1.471864

Kara, Y. S., Sagdinc, S. G., & Esme, A. (2012). Theoretical study on the relationship between the molecular structure and corrosion inhibition efficiency of long alkyl side chain acetamide and isoxazolidine derivatives [journal article]. *Protection of Metals and Physical Chemistry of Surfaces*, *48*(6), 710-721. https://doi.org/10.1134/s2070205112060056

Khaled, K. F. (2009). Experimental and atomistic simulation studies of corrosion inhibition of copper by a new benzotriazole derivative in acid medium. *Electrochimica Acta*, *54*(18), 4345-4352. https://doi.org/http://dx.doi.org/10.1016/j.electacta.2009.03.002

Khalifa, S., AL-abbasi, A., Suliman, M. (2018). Adsorption and Corrosion Inhibition of Mild Steel in Acidic Media by Expired Pharmaceutical Drug. *Journal of Pure & Applied Sciences*, *17*, 1-6.

Khalil, N. (2003). Quantum chemical approach of corrosion inhibition. *Electrochim Acta*, *48*. https://doi.org/10.1016/s0013-4686(03)00307-4

Lee, C., Yang, W., & Parr, R. G. (1988). Development of the Colle-Salvetti correlation-energy formula into a functional of the electron density. *Physical Review B*, *37*(2), 785. http://link.aps.org/doi/10.1103/PhysRevB.37.785

Mahendra Yadav1, Sushil Kumar1, Indra Bahadur2, Deresh Ramjugernath. (2014). Corrosion Inhibitive Effect of Synthesized Thiourea Derivatives on Mild Steel in a 15% HCl Solution *Int. J. Electrochem. Sci.*, *9*, 6529 - 6550.

Martinez, S. (2003). Inhibitory mechanism of mimosa tannin using molecular modeling and substitutional adsorption isotherms. *Materials Chemistry and Physics*, *77*(1), 97-102. https://doi.org/http://dx.doi.org/10.1016/S0254-0584(01)00569-7

Nolan, J. B., P. . (1997). Analgesia and anaesthesia

In A. S. David Skinner, Rodney Peyton & Colin Robertson (Ed.), *Cambridge Textbook of Accident and Emergency Medicine* (pp. 194). Cambridge University Press.

Obot, I. B., Macdonald, D. D., & Gasem, Z. M. (2015). Density functional theory (DFT) as a powerful tool for designing new organic corrosion inhibitors. Part 1: An overview. *Corrosion Science*, *99*, 1-30. https://doi.org/http://dx.doi.org/10.1016/j.corsci.2015.01.037

Pearson, R. G. (1988). Absolute electronegativity and hardness: application to inorganic chemistry. *Inorganic Chemistry*, *27*(4), 734-740. https://doi.org/10.1021/ic00277a030

Perdew, J. P., Burke, K., & Wang, Y. (1996). Generalized gradient approximation for the exchange-correlation hole of a many-electron system. *Physical Review B*, *54*(23), 16533. http://link.aps.org/doi/10.1103/PhysRevB.54.16533

"Lidocaine Hydrochloride (Local)". . Retrieved Aug 26, . (2015).

Robert G. Parr , L. v. S., and Shubin Liu (1999). Electrophilicity Index *J. Am. Chem. Soc.*, *121*(9), 1922-1924.

Sastri, V. S., & Perumareddi, J. R. (1994). Selection of Corrosion Inhibitors for Use in Sour Media. *CORROSION*, *50*(6), 432-437. https://doi.org/doi:10.5006/1.3293521

Scriabine, A. (1999). Discovery and development of major drugs currently in use. In B. A. A. S. Ralph Landau (Ed.), *Pharmaceutical Innovation: Revolutionizing Human Health* (pp. 211). Chemical Heritage Press.

Wazzan, N. A. (2014). DFT calculations of thiosemicarbazide, arylisothiocynates, and 1-aryl-2,5-dithiohydrazodicarbonamides as corrosion inhibitors of copper in an aqueous chloride solution. *Journal of Industrial and Engineering Chemistry*, *26*, 291-308. https://doi.org/http://dx.doi.org/10.1016/j.jiec.2014.11.043

Yang, W., & Mortier, W. J. (1986). The use of global and local molecular parameters for the analysis of the gas-phase basicity of amines. *Journal of the American Chemical Society*, *108*(19), 5708-5711. https://doi.org/10.1021/ja00279a008

Zarrouk, A., Hammouti, B., Dafali, A., Bouachrine, M., Zarrok, H., Boukhris, S., & Al-Deyab, S. S. (2011). A theoretical study on the inhibition efficiencies of some quinoxalines as corrosion inhibitors of copper in nitric acid. *Journal of Saudi Chemical Society*, *18*(5), 450-455. https://doi.org/http://dx.doi.org/10.1016/j.jscs.2011.09.011